Journal of Applied Polymer Science

Effects of star-shaped poly(alkyl methacrylate) arm uniformity on lubricant properties

Joshua W. Robinson,[1] Yan Zhou,[2] Jun Qu,[2] Robert Erck,[3] Lelia Cosimbescu[1]
[1]Pacific Northwest National Laboratory, Richland, Washington
[2]Oak Ridge National Laboratory, Oak Ridge, Tennessee
[3]Argonne National Laboratory, Lemont, Illinois
Correspondence to: L. Cosimbescu (E-mail: lelia.cosimbescu@pnnl.gov)

ABSTRACT: Star-shaped poly(alkyl methacrylate)s (PAMAs) were prepared and blended into an additive-free engine oil to assess the structure–property relationship between macromolecular structure and lubricant performance. These additives were designed with a comparable number of repeating units per arm and the number of arms was varied between 3 and 6. Well-defined star-shaped PAMAs were synthesized by atom transfer radical polymerization (ATRP) via a core-first strategy from multi-functional head-groups. Observations of the polymer-oil blends suggest that stars with less than four arms are favorable as a viscosity index improver (VII), and molecular weight dominates viscosity-related effects over other structural features. Star-shaped PAMAs, as oil additives, effectively reduce the friction coefficient in both mixed and boundary lubrication regime. Several analogs outperformed commercial VIIs in both viscosity and friction performance. Increased wear rates were observed for these star-shaped PAMAs in the boundary lubrication regime suggesting pressure-sensitive conformations may exist. © 2016 Wiley Periodicals, Inc. J. Appl. Polym. Sci. **2016**, *133*, 43611.

KEYWORDS: friction; polyolefins; viscosity and viscoelasticity; wear and lubrication

Received 22 December 2015; accepted 6 March 2016
DOI: 10.1002/app.43611

INTRODUCTION

Lubricant additives are employed to improve the performance, life-span, and energy efficiency of moving mechanical components. In particular, engine oil additives have an essential role in meeting the power performance and fuel economy requirements of modern day automobile standards. Since their initial exploration in the 1930s,[1–3] viscosity modifiers (VM) and/or viscosity index improvers (VII) have been developed to meet the ever increasing demands of the internal combustion engine (ICE) in which environmental stewardship has become a driver toward greater fuel efficiency. Engine oil VII additives are non-uniformly dispersed macromolecules (i.e., oil-miscible polymers) that expand lubricant viscosities via a temperature dependent conformation change (i.e., globular-to-random coil) and/or intermolecular polymer chain entanglements (i.e., concentration dependent).[4,5] In either case, the so called "natural thinning effect" of lubricants is reduced thereby increasing viscosities at higher temperatures. A unit-less viscosity index value (VI) provides a relative viscosity performance metric of liquid lubricants between 40 and 100 °C.[6] In general, higher VIs (>120) are desirable for engine oils and indicate good to excellent viscometric behaviors at or near operating temperatures. Noteworthy, synthetic oils provide competitive to improved lubricant viscosity performances,[7,8] relative to mineral oils containing VMs, at a higher monetarily cost and therefore are limited to specific applications and/or high performance automobiles. Ongoing research in the development of VMs continues to be driven forward mainly to meet the challenges of improving ICE fuel economy and performance of automobiles that utilize non-synthetic motor oils.

A wide variety of VM structures has been previously explored.[9–14] Two such examples include: (1) olefin copolymers (OCP) which are fully saturated carbon-based polymers that thicken oils; and (2) poly(alkyl methacrylate)s (PAMAs) which include fatty and polar esters within the polymer chain.[11,15] VM molar masses can range anywhere from 20 to 500 kDa, in which larger molar masses tend to have a greater influence on shear thickening but are more susceptible to mechanical degradation.[4] Some of the most effective VMs include PAMAs with a

Additional Supporting Information may be found in the online version of this article.

chemical composition of oil-immiscible side-chain moieties (e.g., C_1, alkyl amines, etc.) and oil-miscible alkyl side-chains (i.e., C_{12}–C_{30}) extending from a relatively polar backbone (i.e., methacrylate or methacrylamide).[16,17] The improved viscosity effects have been attributed to the promotion of a globular conformation, via the oil-immiscible moieties at lower temperatures, as well as to greater intramolecular entanglement of the pendant chains.[5,18] With the advent of improved polymerization techniques, researchers from Evonik RohMax Additives GmbHp redesigned PAMAs to elevate various automobile lubricant viscosity indices. Their *comb*-PAMAs (a hybrid of *pseudo*-OCP and PAMA) prepared from radical polymerization of acrylate macromonomers (i.e., transesterification of polyolefin alcohols (1–10 kDa) with methyl acrylates) and short alkyl (C_1–C_4) side-chains yield copolymer-oil blends with competitive thickening efficiencies, viscosity indices, and shear stability properties relative to OCPs (olefin copolymers which are fully saturated carbon based polymers).[11,17] Researchers at the Lubrizol Corporation, pioneers in VMs with star-shaped architectures, developed radial PAMAs that demonstrated resiliency to the high pressures and strong mechanical forces within an automatic transmission.[13,19] Likewise, thesis work by Wright investigated copolymers of star-shaped PAMAs as VMs for gear oils.[20] The Evonik RohMax Additives team also designed star-shaped PAMAs for engine oils and observed superior lubricant performances.[21] These independent studies/patents by industrial leaders support PAMAs, with star-shaped architectures, to be of significant interest within the lubricant VM field. However, fundamental studies that determine which features (i.e., chemical composition and/or architecture) influence lubricant performance (i.e., viscosity, VI, and friction) are scarcely addressed in the open literature.[22–24]

Due to their elevated VIs, desirable thickening efficiencies, enhanced thin film formation properties, and relative mechanical shear degradation resiliency,[25] star-shaped PAMAs are an ideal lubricant additive worth further attention. The purpose of this work was twofold: to develop a star-shaped PAMA oil additive with competitive lubricant performance to at least one commercial VM oil additive (i.e., a performance benchmark); and further understand the structure–property relationships, currently underrepresented in the literature, between macromolecular architecture (e.g., number of arms, molecular weight, etc.) and lubricant performance (i.e., viscosity, VI, friction, and wear). To this end, we prepared star-shaped PAMAs, via a core-first methodology, to target homopolymers containing a unique number of arms (i.e., 3-, 4-, and 6-arms) and comparable arm lengths. For efficient oil thickening properties, molecular weights (M_w) greater than 100 kDa were targeted. The homo-star-shaped PAMAs in this study were dissolved in additive-free engine oil upon which the viscosity indices, friction coefficients, and wear rates were measured. In addition, we also prepared systems with increased non-uniformity utilizing a poly(ethyleneimine) (PEI) macromolecular head-group (average of 3.5 arms) to assess the significance, if any, larger and polar star cores has toward lubricant performance.

EXPERIMENTAL

General Considerations

Copper (I) bromide (CuBr), *N*,*N*,*N*′,*N*″,*N*″-pentamethyldiethylene-triamine (PMDETA), and multi-functional initiators (1,1,1-tris(2-bromoisobutyryloxymethyl)-ethane, pentaerythritol tetrakis(2-bromoisobutyrate), and dipentaerythritol hexakis(2-bromoisobutyrate); α^3, α^4, and α^6) were utilized as received from commercial sources (i.e., Sigma Aldrich, St. Louis, Missouri, USA and TCI America, Portland, Oregon, USA). Poly(ethylenimine) (PEI; $\bar{M}_w = 600$ g/mol, $Đ_M = 1.08$) was purchased from Polysciences, Inc., Warrington, Pennsylvania, USA. α-Bromoisobutyryl bromide was used as received. The monomers (dodecyl methacrylate, DMA, Sigma-Aldrich; and octadecyl methacrylate, OMA, Sigma-Aldrich) were passed through a neutral alumina or silica plug to remove inhibitors. Anhydrous, inhibitor-free tetrahydrofuran (THF, Sigma-Aldrich) was used to prepare the 0.1 *M* CuBr : PMEDTA (1:3) solution. Reaction equipment was oven dried, placed under vacuum while cooling, and backfilled with argon flowing through a tube filled with activated silica gel orange (drying agent). Group III base oil (4Yubase; Y4) was used to create a baseline for viscosity and friction measurements, clean in between measurements, and prepare lubricant mixtures with synthesized polymers. Additive free Y4 oil was kindly donated by Afton Chemical Corporation, Richmond, Virginia, USA and by Evonik Oil Additives USA, Inc., Horsham, Pennsylvania, USA. Benchmarks 1 and 2 are commercial lubricant VM kindly donated by The Lubrizol Corporation, Wickliffe, Ohio, USA and Evonik, respectively, and were employed here as comparative examples.

Characterization

Nuclear magnetic resonance (NMR) spectra were obtained using an Agilent-Oxford 500 MHz spectrometer at the following frequencies: 499.8 MHz (^{1}H) and 125.7 MHz (^{13}C{^{1}H}). The chemical shifts are reported in delta (δ) units, parts per million (ppm) downfield from tetramethylsilane and coupling constants are reported in Hertz (Hz). Samples were prepared in deuterated chloroform ($CDCl_3$, Sigma-Aldrich) containing tetramethylsilane (TMS, 0.3 − 1%, vol/vol). Post-functionalized PEI ($\alpha^{3.5}$) was analyzed by time-of-flight mass spectrometry (ToF-MS). Relative molar mass distributions were obtained by size exclusion chromatography (SEC) analysis. The molar masses were determined relative to the elution volumes of linear poly(-methyl methacrylate) standards pushed through two columns of Jordi Gel DVB Mixed bed (250 mm × 10 mm) in THF (mobile phase) and detected via a refractive index detector (Jordi Labs, Mansfield, Massachusetts, USA).

Preparation of $\alpha^{3.5}$ [26]

A reaction flask containing reagent grade toluene (Fisher Scientific International Inc., Pittsburgh, Pennsylvania, USA) (50 mL) and PEI (1.28 g, 2.1 mmol; ~3.5 eq. —NH_2 per mol) was placed into an ice bath for ~15 min. A 2.0 *M* NaOH/H_2O solution was poured into the reaction flask and stirred vigorously. Then 2.0 mL of α-bromoisobutyryl bromide (0.16 mol; ~2 eq. per amine) was transferred into the reaction flask and the reaction was allowed to warm to r.t. for ~12 h. To reduce the biphasic nature of this reaction, 15 mL of reagent grade

acetonitrile (Fischer Scientific) was added. After an additional 12 h, excess H_2O was added and the pH was adjusted to ~1 with the slow addition of concentrated hydrochloric acid. The organics were extracted in ethyl acetate (Fisher Scientific) (3× 150 mL) and dried over anhydrous sodium sulfate (Na_2SO_4, Sigma-Aldrich). The solvent was removed in vacuo to yield a viscous yellow oil which became a solid under high vacuum. This crude material was purified by chromatography on silica gel with a gradient elution of 0 − 20% MeOH/DCM (Fisher Scientific) (vol/vol). The volatile organics were once again removed by vacuum techniques. A white and fluffy crystalline material was collected with a gravimetric mass of 1.07 g (45% yield).

$\alpha^{3.5}$. ^{1}H-NMR ($CDCl_3$, 500 MHz): δ 7.80 − 7.07 (m, 2.48H), 7.00 − 6.26 (m, 2.01H), 4.29 − 3.31 (m, 7.37H), 3.31 − 2.57 (m, 4.63H), 2.10 (s, 1.02H), 2.06 − 1.89 (m, 11.33H), 1.47 (s, 2.00H). $^{13}C\{^1H\}$ NMR ($CDCl_3$, 125 MHz): δ 181.3, 175.8, 172.7, 171.1, 72.1, 61.2, 57.0, 53.8, 51.0, 48.8, 46.4, 39.0, 32.8, 32.3, 27.4, 22.7, 21.0. HRMS (ESI) illustrate molecular weight distributions which do not show the parent MW, but do show evidence of bromoisobutyrate functionalization by the loss of fractions with $m/z = 193$ (Supporting Information S1). Lower molecular weight distribution series: 593.02, 786.01, 979.01, 1172.00, 1365.01; higher molecular weight series: 827.06, 1020.05, 1213.05, 1406.04, 1599.03, 1792.04, 1985.04 m/z; ($\Delta m/z = 192.99$, $[C_6H_{12}BrNO]$ requires 193.01 [^{79}Br] and 195.01 [^{81}Br]).

Polymerization. [27]

The monomer and multi-functional initiator (α^3, $\alpha^{3.5}$, α^4, or α^6) were transferred into a 2-neck reaction flask fitted with an air condenser and rubber septum. The reaction flask was degassed via vacuum-argon cycles (3×) and left under vacuum for ~30 min. A fresh 0.1*M* CuBr:PMDETA/THF solution was prepared in a Schlenk round bottom flask under argon. The reaction flask was backfilled with argon and heated to ~70 °C. The catalyst solution was injected into the reaction mixture and the external sand bath's temperature was increased to ~120 °C, over ca. 30 min. The reaction mixture changed from green to amber and started becoming viscous in ca. 60 min. An aliquot of the reaction mixture was periodically analyzed by ^{1}H-NMR to monitor the progression of the polymerization. Typically, the reaction reached a 70% conversion within 2 − 3 h and was allowed to run for ca. 12 h to reach 85–90% conversion. The reaction flask was opened to the air which effectively terminated the polymerization. The crude polymer was refluxed in acetonitrile, cooled to r.t., and then the solvent was decanted off. This process was repeated until a clean polymer with less than 5 mol % of monomer was obtained, typically three times.

α^3-PA_{12}MA (Analog 2). ^{1}H-NMR ($CDCl_3$, 500 MHz): δ 3.91 (b, 2.00H), 2.06 − 1.70 (m, 2.01H), 1.70 − 1.52 (m, 2.63H), 1.27 (b, 19.88H), 1.01 (b, 1.38H), 0.88 (t, 4.64H, $J = 5.0$ Hz). $^{13}C\{^1H\}$ NMR ($CDCl_3$, 125 MHz): δ 177.9, 177.5, 176.8, 65.1, 54.4, 52.6, 45.2, 44.9, 32.1, 29.8, 29.7, 29.5, 29.4, 28.3, 28.3, 26.2, 22.8, 18.4, 16.7, 14.2. SEC (PMMA cal.): $\bar{M}_n^{app} = 103.6$ kg/mol, $\bar{M}_w^{app} = 295.0$ kg/mol, $Đ_M = 2.8$, bimodal.

α^3-PA_{18}MA (Analog 3). ^{1}H-NMR ($CDCl_3$, 500 MHz): δ 6.09 (s, 0.07H), 5.54 (s, 0.09H), 4.13 (t, 0.14H, $J = 7.5$ Hz), 3.92 (b, 2.00H), 2.07 − 1.70 (m, 2.41H), 1.67 − 1.54 (m, 1.96H), 1.26 (b, 24.20H), 1.14 (b, 0.46), 1.02 (b, 1.26H), 0.89 (t, 3.70H, J = 7.5 Hz). SEC (PMMA cal.): $\bar{M}_n^{app} = 79.5$ kg/mol, $\bar{M}_w^{app} = 122.3$ kg/mol, $Đ_M = 1.5$.

$\alpha^{3.5}$-PA_{12}MA (Analog 4). ^{1}H-NMR ($CDCl_3$, 500 MHz): δ ^{1}H NMR ($CDCl_3$, 500 MHz): δ 6.09 (s, 0.09H), 5.54 (s, 0.09H), 4.14 (t, 0.14H, $J = 7.5$ Hz), 3.92 (b, 2.00H), 2.08 − 1.70 (m, 2.13H), 1.70 − 1.51 (m, 2.30H), 1.28 (b, 16.02H), 1.02 (b, 1.01H), 0.89 (t, 4.39H, J = 5.0 Hz). $^{13}C\{^1H\}$ NMR ($CDCl_3$, 125 MHz): δ 177.9, 177.5, 176.9, 125.2, 65.1, 54.2, 45.3, 44.9, 32.1, 29.8, 29.7, 29.5, 29.4, 28.4, 28.3, 26.2, 22.8, 18.4, 16.7, 14.2. SEC (PMMA cal.): $\bar{M}_n^{app} = 179.8$ kg/mol, $\bar{M}_w^{app} = 396.2$ kg/mol, $Đ_M = 2.2$.

α^4-PA_{12}MA (Analog 5). ^{1}H-NMR ($CDCl_3$, 500 MHz): δ 6.09 (s, 0.08H). 5.54 (s, 0.09H), 4.13 (t, 0.12H, $J = 7.5$ Hz), 3.91 (b, 2.00H), 2.10 − 1.69 (m, 2.10H), 1.69 − 1.52 (m, 2.14H), 1.27 (b, 16.49H), 1.01 (b, 1.19H), 0.89 (t, 4.07H, J = 7.5 Hz). $^{13}C\{^1H\}$ NMR ($CDCl_3$, 125 MHz): δ 177.9, 177.5, 176.8, 125.2, 65.1, 54.3, 52.5, 45.3, 44.9, 32.1, 29.8, 29.7, 29.5, 29.4, 28.4, 28.3, 26.2, 22.8, 18.4, 16.7, 14.2. SEC (PMMA cal.): $\bar{M}_n^{app} = 112.1$ kg/mol, $\bar{M}_w^{app} = 159.6$ kg/mol, $Đ_M = 1.4$.

α^6-PA_{12}MA (Analog 6). ^{1}H-NMR ($CDCl_3$, 500 MHz): δ 6.09 (s, 0.08H), 5.54 (s, 0.08H), 4.14 (t, 0.11H, J = 7.5 Hz), 3.92 (b, 2.00H), 2.07 − 1.70 (m, 2.41H), 1.67 − 1.54 (m, 1.96H), 1.27 (b, 15.26H), 1.01 (b, 1.16H), 0.89 (t, 3.89H, $J = 5.0$ Hz). $^{13}C\{^1H\}$ NMR ($CDCl_3$, 125 MHz): δ 177.9, 177.5, 176.8, 125.2, 65.1, 54.2, 53.5, 45.3, 44.9, 32.1, 29.8, 29.7, 29.7, 29.5, 29.4, 28.4, 28.3, 26.2, 22.8, 18.4, 16.7, 14.2. SEC (PMMA cal.): $\bar{M}_n^{app} = 152.9$ kg/mol, $\bar{M}_w^{app} = 265.1$ kg/mol, $Đ_M = 1.7$.

Tribology Investigations

Polymers were dissolved into 4Yubase (Y4) at a concentration of 2% wt/wt and resulting blends were measured by resonance and spindle viscometers to determine dynamic viscosity (centipoise, cP = mPa • s) at 10, 23, 40, and 100 °C. The viscosity data was converted into centistokes (cSt = $mm^2 \bullet s^{-1}$) by dividing the centipoise value by the density of the blend (0.832 g • cm^{-3} at r.t.). The densities of the blends were roughly the same, independent of the polymer used. A Brookfield digital (LVDV-E) spindle viscometer was fitted with a cooling/heating jacket that was continuously flowing with oil supplied by an external cooling/heating bath that regulated the jacketed temperature at 40 and 100 °C. A rotating spindle (0.3 − 100 RPM) was submerged into the blended oil at the regulated temperatures for 30–60 min. The dynamic shear was reported on the digital screen with a respective torsion percent. The cP value with the highest torsion percent was used for VI calculations. An on-line calculator[28] well accepted by experts in the field, was used to generate VI values. The Brookfield viscometer was used only for determining the kinematic viscosity (KV) at 40 and 100 °C. A Viscolite® 700 (VL7-100B-HP) viscometer was used to determine the KV of the blends at 10 and 23 °C. The oil's internal temperature was regulated by an external circulating water bath (10 and 23 °C) for 30–60 min. For high-temperature high-shear measurements, a Tannas TBS viscometer was used to measure the viscosity of the blends at 150 °C while under a shear rate of 1×10^6 s^{-1} (ASTM D4683). A reference oil (R-350, 2.617 cP at 150 °C) was utilized to calibrate the instrument with a specific spindle height as well as provide a linear slope (RPM vs. shear rate) to interpolate the

viscosities of the blended oils. A variable load-speed bearing tester (VLBT) was utilized to obtain Stribeck curves at room temperature.[29] A 50 N normal load was applied through a stiff spring. A 25.4 mm diameter rotating bar of AISI 8620 alloy steel was used to rotate against a 25.4 mm square coupon of A2 tool steel. The coupon holder was filled with lubricants at the beginning of each test. The speed cycle started from 1.7 m/s and reduced to 0.2 m/s at 0.1 m/s per step. Each step lasted 10 s, and three cycles for a total of 480 s were performed for each sample. The friction results from the 1st cycle served as the running-in period with data unused while the results from the 2nd and the 3rd cycle were averaged and plotted. The surfaces of the coupon and the bar were cleaned with isopropyl alcohol before each test. Neat Y4 was used before testing each blend to obtain a baseline. A Phoenix-Tribology Plint TE77 reciprocating tribometer was used to measure friction and wear at 100 °C of selected lubricants. An AISI 52100 steel ball of 10 mm diameter was used to slide against a CL35 gray cast iron flat, which was polished using 600 grit grinding paper. At 100 °C, the tests were performed under a 100 N normal load for 1000 m. The oscillation frequency was at 10 Hz and the stroke length was 10 mm. Two replicates were carried out for each lubricant. The wear rates of the cast iron flats were measured using a Wyko NT9100 interferometer.

RESULTS AND DISCUSSION

Strategy

Star-shaped PAMAs are attractive candidates as lubricant additives due to their architecture and synthetic versatility important in manipulating properties such as thickening efficiency, thin-film forming, enhanced shear stability, and raised VI values. In general, star-shaped polymers may be prepared by living and/or controlled polymerization techniques via a core-first, coupling-onto, or arm-first methodology.[27]

The core-first method provides a route toward well-defined star-shaped homo- and copolymers which utilizes multi-functional initiators (α^n). The arms are grown from this central core while under controlled polymerization conditions. The core-first strategy utilizing anionic polymerization (AP),[30] metal-catalyzed living radical polymerization,[31] nitroxide-mediated polymerization (NMP),[32] reversible addition-fragmentation chain-transfer (RAFT),[33] and atom transfer radical polymerization (ATRP)[34] have been previously investigated by other groups. For our needs, ATRP appeared to be the best choice: a well-established controlled polymerization technique that does not introduce sulfur into high quality petroleum oils and affords an opportunity to investigate arm uniformity effects toward the performance of engine oils, particularly viscosity.

Synthesis

The preparation of 3-,4-,6-arm star-shaped poly(dodecyl methacrylate) (α^3-, α^4-, α^6-$PA_{12}MA$), ~3.5-arm ($\alpha^{3.5}$-) $PA_{12}MA$, and 3-arm poly(octadecyl methacrylate) (α^3-$PA_{18}MA$) was achieved via a modified ATRP synthesis originally described for the core-first polymerization of styrene[35] and methyl acrylate[36] (Scheme 1). Due to the significant role that arm length of star-shaped polymers has toward rheology,[23] we targeted star-shaped PAMAs with comparable arm lengths by controlling the number of repeating units (n) per arm via the monomer to initiator feed ratio ($[M]_0/[I]_0$; Table I, analogs 2, 5, and 6). In addition, we targeted a lower number of repeating units per arm for α^3-$PA_{12}MA$ (analog 1) as a comparison platform to briefly investigate the role arm length plays on viscometric properties. An analog with a different pendent length was targeted (α^3-$PA_{18}MA$, analog 3) to determine what influence the intramolecular chain entanglement of the pendant side-chains might have toward viscosity and friction performance. We also prepared $\alpha^{3.5}$-$PA_{12}MA$ (i.e., greater polydispersity, analog 4) from a low molecular weight poly(ethyleneimine) (PEI; $\bar{M}_w \approx 600$ Da) post-modified with α-bromoisobutyryl bromide, to investigate how a polar multi-functional initiator with poor uniformity in the number of arms, architecture, and molar masses may have on lubricant properties. Finally, we explored the preparation of α^3-$PA_{12}MA$ in group III oil (4Yubase; Y4) at 30% wt/wt to determine amenability to scale up and industrial processes (analog 7). Except for the latter, unreacted monomer was readily removed via acetonitrile washings providing a clean polymer system with equal or less than 5 mol % (as determined by ^{1}H-NMR) of the respective monomer remaining.

General Synthetic Method. A multi-functional core (i.e., α^3, α^4, α^6, or $\alpha^{3.5}$) was combined with inhibitor free dodecyl or octadecyl methacrylate (DMA or OMA, respectively) and degassed via three cycles between a vacuum pump and positive argon feed. A 0.1*M* copper (I) bromide (CuBr) solution of uninhibited tetrahydrofuran (THF) and *N,N,N′,N″,N″*-pentamethyldiethylene-triamine (PMDETA) was prepared separately. A 10 mol % equivalence of CuBr solution to multi-functional core was injected into the core/monomer solution initially heated to 70 °C. Then the external temperature was increased to 120 °C for the duration of the polymerization. Precipitation from dichloromethane into acetonitrile was utilized to purify the respective polymers (3-, ~3.5-, 4-, 6-arm star-shaped poly(dodecyl methacrylate) (α^3-, $\alpha^{3.5}$-, α^4-, α^6-$PA_{12}MA$) and 3-arm poly(octadecyl methacrylate) (α^3-$PA_{18}MA$)).

Characterization

Proton nuclear magnetic resonance spectroscopy (^{1}H-NMR) was utilized to determine the conversion of monomer into polymer via an apparent frequency shift (δ: 4.13, triplet, to 3.92, broad, ppm) and respective integration changes between these alpha ester methylene peaks. Spectral peaks related to the multi-functional head-group were not detectable due to overlapping peaks in the saturated carbon region and its relative low concentration. Therefore, end-group analysis was not possible and an approximate number of repeating units (n), related to each arm, was calculated via the conversion multiplied by the relevant $[M]_0/[I]_0$. From this, the number-average molar mass $\bar{M}_n$ was determined, see Table I. The n for each arm ranges from 117 to 180 and the respective $\bar{M}_n$ ranges from 90.3 to 271.8 kDa. In particular, analogs 2, 4, 5, and 6 have n within 12 repeating units of each other, according to ^{1}H-NMR analysis.

SEC molar fraction chromatograms illustrate mono-modal dispersed star-shaped PAMAs were obtained (Figure 1) with the exception of analogs 1 and 2. Overall, the molecular weight fractions support an apparent weight-average molecular weight

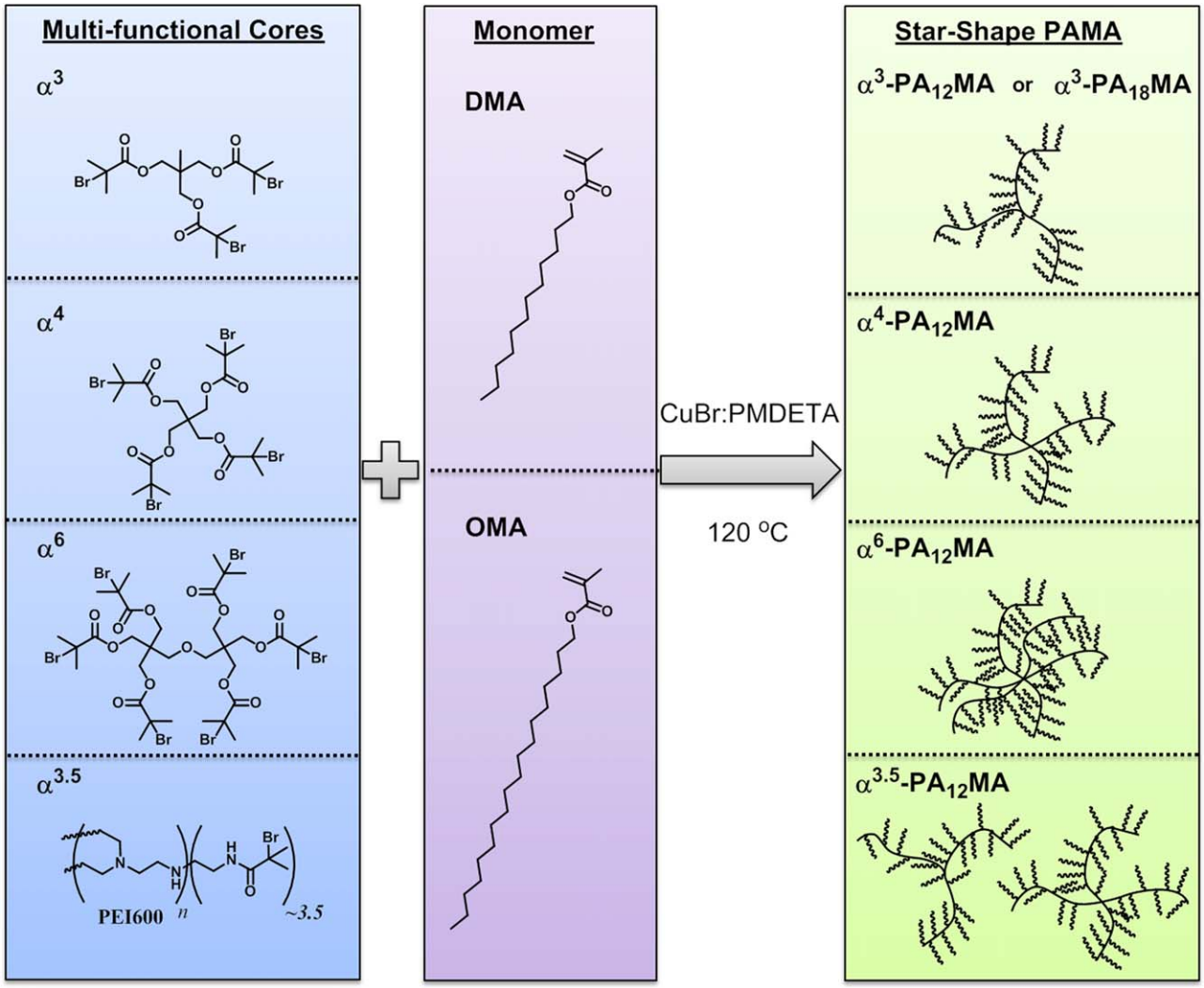

Scheme 1. General synthetic approach towards preparing star-shaped PAMAs. [Color figure can be viewed in the online issue, which is available at wileyonlinelibrary.com.]

($\bar{M}_w^{app}$) range of 78.5 − 295.0 kDa with moderate to high molar dispersities ($Đ_M \approx 1.4 - 2.8$; Table I). Analog 1 and 2's $\bar{M}_w^{app}$ and $Đ_M$ values were elevated due to a higher molar mass fraction with peak maxima (M_p) of 692 and 1596.9 kDa, respectively, whereas the more abundant molar fraction M_p was 93.7 and 100.1 kDa. Our reactions were conducted either as neat or as highly concentrated monomer solutions to minimize unreacted arms potentially caused by the steric congestion of the bulky repeating units (i.e., long pendant groups) surrounding the core. Unfortunately, this synthetic strategy provided greater opportunities for macromolecular coupling, such as star–star coupling, which resulted in higher molar mass fractions in two instances. Noteworthy, analogs 3 through 6 were conducted under similar conditions and the SEC eluent chromatogram does not illustrate a higher weight fraction as a shoulder peak suggesting some other variable besides concentration contributed to macromolecular coupling such as temperature and duration. Furthermore, a α^3-$PA_{12}MA$ was prepared in 4Yubase (Y4) at a 30% wt/wt concentration; this analog molecular weight is the lowest of all its α^3 counterparts, suggesting that heat dissipation and concentration play a significant role in the reaction outcome.

Viscosity Performance of PAMA–Oil Blends

It should be noted here that the authors are aware of industry protocols in comparing the performance of various lubricant packages. One such method includes varying the formulation of different lubricants so that the kinematic viscosity (KV) at a set temperature (i.e., 40, 100, or 150 °C) is equivalent. This requires in-depth formulation studies incorporating various lubricant additives (e.g., foam inhibitors, pour point depressants, friction modifiers, antioxidants, etc.) and large amounts of VM material to optimize VI performance of a given stock. We on the other hand are comparing structural differences among analogs and how that impacts VI, so our study keeps the concentration of the polymer constant at 2% by weight (wt/wt). Future optimization work will include comparisons of polymers at a matched KV temperature. Another important mention is that the benchmarks are not used as references to draw conclusions about architectural differences, but rather to set a performance

Table I. Molecular Weight Characterization of Star-Shaped PAMAs

			^{1}H NMR[b]			SEC[c]		
Analog	Composition	$[M]_0/[I]_0$[a]	Conv. %[d]	n[e]	$\bar{M}_n$(kg/mol)[f]	$\bar{M}_n^{app}$ (kg/mol)	$\bar{M}_w^{app}$ (kg/mol)	D_M[g]
1	α^3-$PA_{12}MA$	133	88	117	90.3	89.5	245.4	2.7
2	α^3-$PA_{12}MA$	205	82	168	129.8	103.6	295.0	2.8
3	α^3-$PA_{18}MA$	161	87	140	143.6	79.5	122.3	1.5
4	$\alpha^{3.5}$-$PA_{12}MA$	230	73	168	151.8	179.8	396.2	2.2[h]
5	α^4-$PA_{12}MA$	200	87	173	178.3	112.1	159.6	1.4
6	α^6-$PA_{12}MA$	200	90	180	271.8	152.9	265.1	1.7
7	α^3-$PA_{12}MA$	158	74	117	90.8	51.3	78.5	1.5

[a] The actual monomer to arm initiator feed ratios $[M]_0/[I]_0$ determined by gravimetric mass.
[b] Nuclear magnetic resonance (NMR) spectrometry with tetramethylsilane (TMS, $\delta = 0.00$) as an internal reference for proton (^{1}H) analysis in deuterated chloroform ($CDCl_3$)
[c] Apparent number-average molecular weight ($\bar{M}_n^{app}$) and apparent weight-average molecular weight ($\bar{M}_w^{app}$) were determined via size exclusion chromatography (SEC) against poly(methy methacrylate) standards.
[d] Percent of conversion (Conv. %).
[e] The number of repeating units (n) per arm.
[f] Number-average molar mass ($\bar{M}_n$) of the star-shaped polymer.
[g] Molar dispersity ($Đ_M$) was calculated from $\bar{M}_w^{app}/\bar{M}_n^{app} = Đ_M$.
[h] Expected elevation in non-uniformity caused by the hyper-branched core, PEI600.

standard. The goal of this study was not only to understand structure–property relationships for this particular class of compounds, but also provide viable candidates with competitive performance. One of the performance metrics (VI or friction) of the blended oil–polymer analogs is expected to be comparable if not higher than at least one of the benchmarks. Thus, all analogs including benchmark 1 (Bench. 1) and benchmark 2 (Bench. 2) were prepared at the same concentration of 2% in 4Yubase (Y4). Note, analog 1 thru 7 in Table II correspond respectively Table I annotation. Analog 7's 2% wt/wt concentration was adjusted in consideration of the relative conversion (74%) of the polymerization in which the unreacted monomer was considered to be part of the oil's mass. The dynamic viscosity (centipoise; cP) of the neat oil and PAMA-oil blends were measured by resonance (10 and 23 °C) and spindle (40 and 100 °C) viscometers at controlled temperatures. These values were converted into kinematic viscosity (KV: centistokes, cSt) and are reported in Table II. The determined KVs at 40 and 100 °C were utilized to generate the VI values via an online calculator. Another significant value for lubricant evaluation and the subsequent determination of the oil grade it falls in,[37] is a high-temperature high-shear test (HTHS), which imposes a low viscosity limit on the final oil and determines the last number of the viscosity grade (i.e., 20 in the 0W20).[38] This test is performed at 150 °C which is presumed to be approaching the highest temperature and shear boundary the lubricant may experience during engine operation (ASTM DS-62).

Formulations prepared with benchmark 1 at 2% wt/wt significantly increased the VI of Y4, however it also increased the lower temperature viscosity. A significant increase in viscosity at 40 °C is generally undesirable for engine oil applications. In contrast, benchmark 2 increased the 40 °C viscosity to a lesser extent, while achieving an even higher VI. The blends prepared with our star-shaped PAMAs at 2% wt/wt followed the same trend as benchmark 2 in which the additive did not overwhelmingly increase the viscosities at lower temperatures but significantly increased the VI of Y4. The VIs ranked in the following order: Bench. 2 > Analog 2 > Analog 4 > Analog 6 > Analog 1 = Bench. 1 > Analog 5 > Analog 7 = Analog 3 > Y4.

Deciphering molecular features that demonstrated the greatest effect toward lubricant VIs was convoluted due to irregularities in the polymer architectures (i.e., $Đ_M \geq 1.4$). According to traditional understanding, the greater size/conformational changes that a polymer experiences with temperature, the greater the VI. We are monitoring VI and viscosity changes with respect to the temperature of the aforementioned polymer analogs mixed in base oil to assess potential conformational changes in these polymers with increasing temperature. To that end, our expected trend, as far as VI is concerned, is that the VI should decrease from analogs 2, 4, 5, and 6, as the number of arms increases. At the same time, we expect molecular weight to follow the opposite trend, provided that reactions occurred as expected: 6 > 5 > 4 > 3 > 2. In other words, when the molecular weight does not greatly differ, then the conformational freedom of the stars will dictate VI performance. On the other hand, if the conformational freedom of the stars is limited, then VI and low temperature viscosity performance should be dominated by the molecular weight. In support of this understanding, Wright's dissertation thesis of core-first star-shaped PAMAs illustrate a slight decrease in VI when the number of arms ($n = 3$, 4, and 5) increased at a constant molecular weight of about 20 kDa.[20] This hypothesis, at first glance, opposes work by Fetters *et al.* in which they demonstrated a 20% loss in viscosity of star-shaped poly(isoprene)s from 4- to 3-arms, at high concentrations (50% wt/wt), that they attributed to a decrease in intermolecular arm entanglements. However, the ideal concentration for our application is less than 5%, which should significantly reduce intermolecular arm entanglements and afford conformational dependent VI responses. Thus any significant change in VI may be accredited to intramolecular

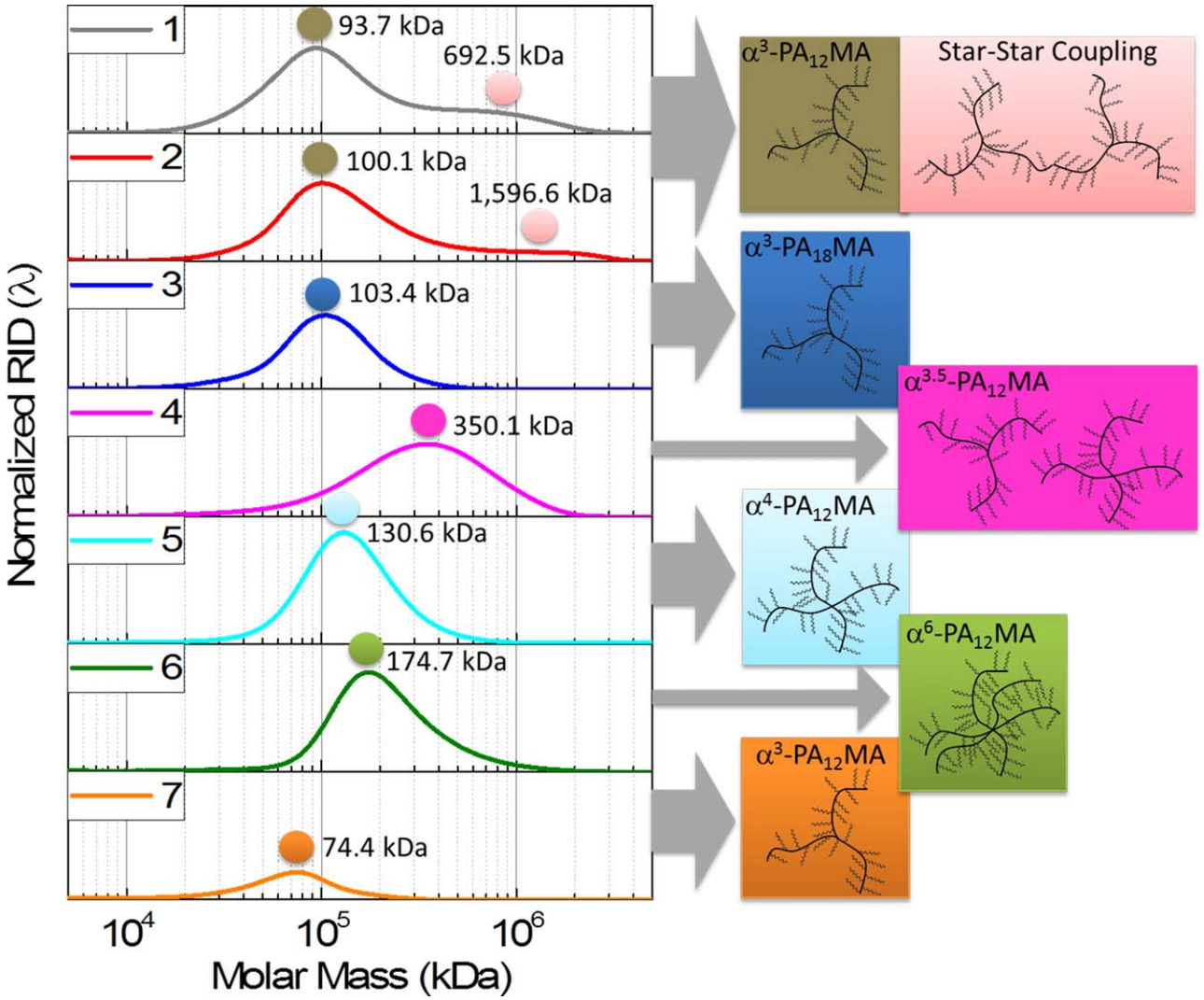

Figure 1. Stacked SEC molar mass distribution curves of Analogs 1 − 7 (left) and cartoon image of predicted structures (right). Numbers near bubbles are molecular weights of the peak maxima (M_p). [Color figure can be viewed in the online issue, which is available at wileyonlinelibrary.com.]

conformational changes. At the same time, we cannot rule out molecular weight influences on the viscosity behavior and must account for this variable during our interpretations.

As previously mentioned, we targeted four star-shaped $PA_{12}MA$s (i.e., Analog 2, 4, 5, and 6) to contain relatively similar number of repeating units ($\Delta n \leq 12$) within the arms while varying the number of arms from 3 to 6. The VIs of the respective blends are 204, 198, 187, and 190, with the highest being the 3 arm analog. It does appear that the number of arms has a small but consistent effect on VI. However, this understanding is complicated by the molecular weight influence which inherently increases with additional arms. To add another degree of difficulty, in the case of analogs 1 and 2, star-cross coupling products are suspected, as indicated by the bimodal mass distribution shown in Figure 1. The coupled star fractions apparently have a larger influence on viscosity and VI behavior than uncoupled star analogs such as analog 7. What is surprising about these results is the significant change in VI although the relative concentration of the coupled to uncoupled stars is significantly lower. For example, the apparent molar fraction M_ps of analog 1, 2, and 3 are relatively similar but demonstrate significantly different VI behaviors. Of these 3-arm analogs, analog 3 has the higher $\bar{M}_n$, as determined by ^{1}H-NMR analysis, due to the elongated pendant group but has the lowest VI performance of them. Out of analogs 1, 2, 3, 5, and 6, analog 6 was determined by ^{1}H-NMR and SEC analysis to have the greatest $\bar{M}_n$ and M_p, respectively, but does not outperform analog 2. Noteworthy, analog 4 has the greatest apparent M_p out of the mono-modal series and demonstrated competitive VI performance to analog 2. This suggests that increased non-uniformity may be beneficial for VI behavior. Although it is not possible to decouple influences from the number of arms or molecular weight toward VI performance, subtle differences of the viscometric properties between low and high temperatures may shed some light on this matter.

Indeed, it appears that the higher molecular weight analog has a higher VI. That however still does pose the question of

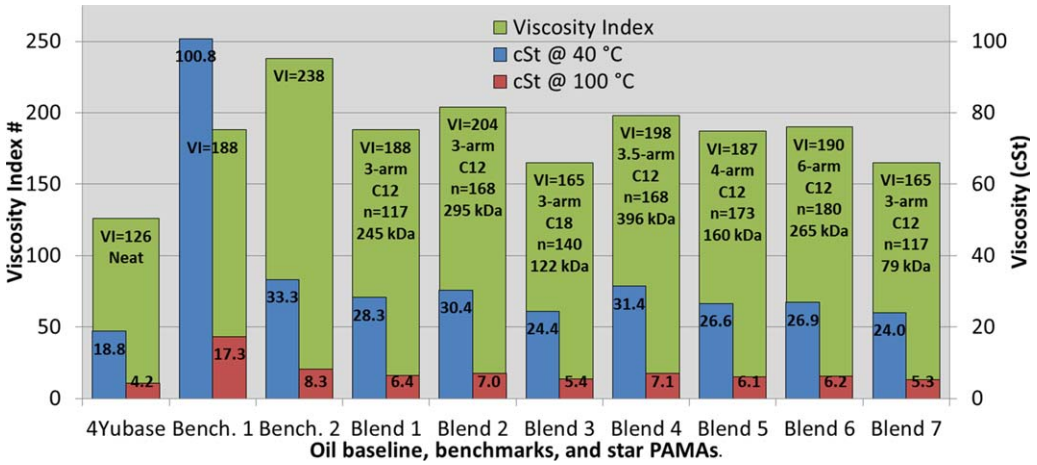

Figure 2. Viscosity data as measured via a spindle viscometer and calculated VI values.[28] [Color figure can be viewed in the online issue, which is available at wileyonlinelibrary.com.]

whether the arm length or weight itself plays the major factor. That can be answered by carefully analyzing the viscosity values at low and high temperatures. It appears that both analogs start off with similar viscosities at 10 °C and even 23 °C; however the longer chain-analog appears to have a greater influence at high temperature, which may have to do with the coil expansion ability of a star–star system. This side-by-side comparison seems to suggest that the expansion potential of the hydrodynamic volume, as related to arm length, is more important than weight itself. Overall, our independent investigations support the significance that arm-length, over molecular weight and number of arms, has toward VI behavior.

Analogs 3 and 7 have a similar number of repeating units, 140 and 117, respectively, with the same number of arms and their molecular weight distributions are mono-modal; therefore they provide the best study candidates of the effect that the pendant chain length has on the viscosity behavior. However, we are faced with the same challenge of decoupling the effects of molecular weight versus structure. Analog 3 has a much higher molecular weight than analog 7, yet both have a similar VI of 165, which is in contrast to our prediction of molecular weight influence. This suggests that the longer pendant chain has no beneficial effect toward the elevation of VI.

Overall, the star-shaped polymers show a strong dependence on molecular weight and arm length. Polymer fractions which shift the molecular weight to the right seem to have a substantial influence on viscosity and VI, however may be more susceptible to mechanical shear and therefore were not targeted in this study. Although none of the analogs outperformed benchmark 2, they all outperform benchmark 1, in that the VI is comparable or higher as well as they all have a lower KV profile at 40 °C. For fuel economy, a minimal KV $\leq$ 40 °C is extremely

Table II. Measured Kinematic Viscosity (cSt) Values and Respective Calculated Viscosity Indices (VIs)

	Resonance Viscometer (cSt)[d]		Spindle Viscometer (cSt)[d,e]			HTHS (cSt)[d,g]
Analog[a,c]	10 °C	23 °C	40 °C	100 °C	VI	150 °C
4Yubase	66.7	37.3	18.8	4.2	126	1.56
Bench. 1	181.6	115.7	100.8	17.3	188	n.d.
Bench. 2	94.2	56.6	33.3	8.3	238	2.25
1 (α^3/C_{12})	88.8	52.0	28.3	6.4	188	n.d.
2 (α^3/C_{12})	87.6	52.0	30.4	7.0	204	1.98
3 (α^3/C_{18})	81.6	48.6	24.4	5.4	165	1.92
4 ($\alpha^{3.5}/C_{12}$)	87.1	53.6	31.4	7.1	198	2.17
5 (α^4/C_{12})	86.5	50.1	26.6	6.1	187	2.01
6 (α^6/C_{12})	88.8	52.0	26.9	6.2	190	2.07
7 (α^3/C_{12})	82.7	46.9	24.0	5.3	165	n.d.

[a] 4Yubase = 0.83 g/cm^3.
[b] 2% wt/wt polymer-Y4 density = 0.832 g/cm^3.
[c] Annotation corresponds to Table I, analog 1 = analog 1 at 2% wt/wt.
[d] cSt=cP/ρ
[e] Viscosity indices were generated via online calculator.[28]
[f] High-temperature high-shear (HTHS) was performed according to ASTM D4683.
[g] Not determined (n.d.).

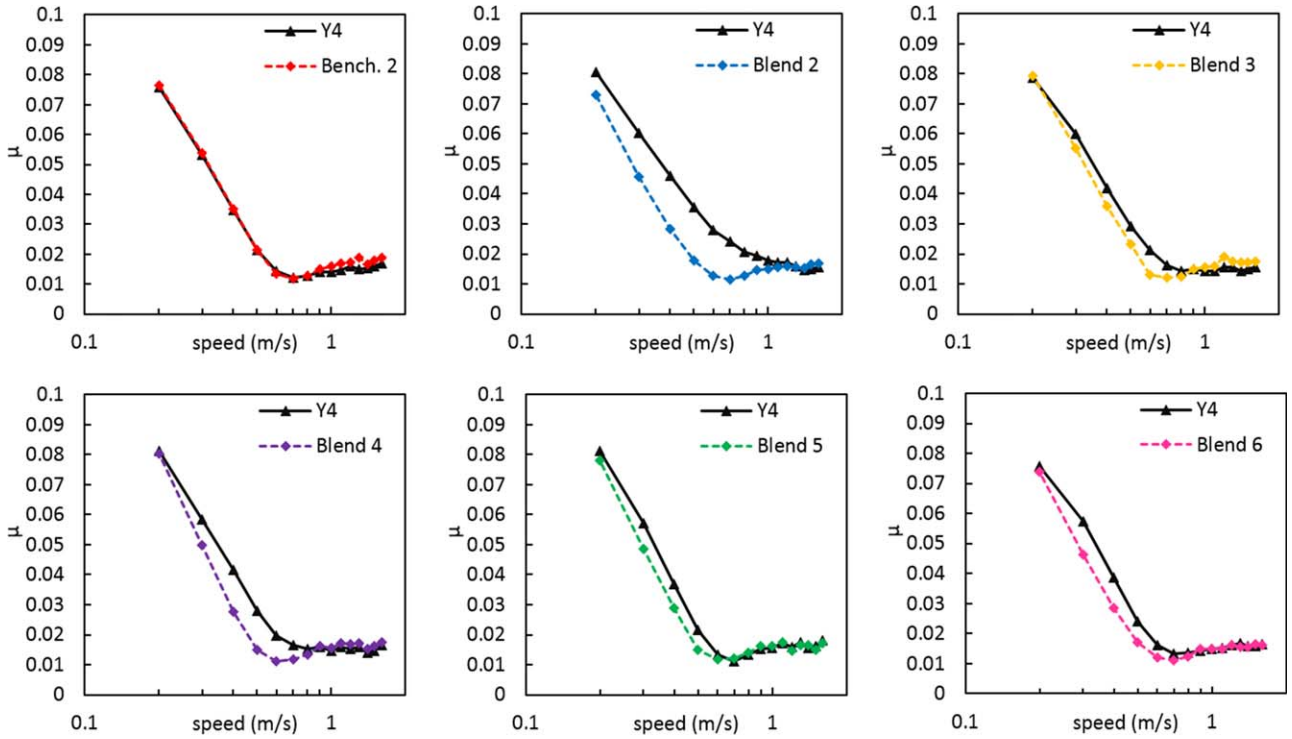

Figure 3. Stribeck curves of Bench. 2 (2 wt %) and analogs 2 − 6 (2 wt %) at room temperature. [Color figure can be viewed in the online issue, which is available at wileyonlinelibrary.com.]

desirable. From that perspective, analogs 5 and 6 (4- and 6-arm analogs, respectively) appear to have a high VI while maintaining the lowest KV at 40 °C, and therefore might be the more attractive candidates.

Friction Performance of PAMA–Oil Blends

Increased fuel efficiency of ICEs has been observed when thin or low viscosity (e.g., SAE 0W20) lubricants are employed.[38,39] The downside is that as the lubricant becomes even thinner with temperature, increased contacts between hard asperities occur more frequently leading to a promotion in friction and wear. Friction modifiers, in part, are generally added to mitigate this effect.[40] In a couple of examples, VMs (such as comb PAMAs copolymers)[41] have been demonstrated to reduce friction by promoting thin film formation on sliding asperities.[42] In an effort to elucidate the effects arm uniformity and core structure may demonstrate towards friction performance, as well as probe the performance of our analogs against commercial benchmarks, Stribeck curves from selected blends were obtained by a variable-load journal bearing tester (VLBT) and the wear rates were measured via Plint tribometer (refer to Tribology investigations within the Experimental Section for more details).

Initial VLBT friction studies were performed on benchmark 2 and analogs 2 − 6 at room temperature, as shown in Figure 3. The neat Y4 curves were the average of two Y4 tests performed before and after each blend. As described earlier, benchmark 2 and analogs 2 − 6 have relatively comparable viscosities at 23 °C

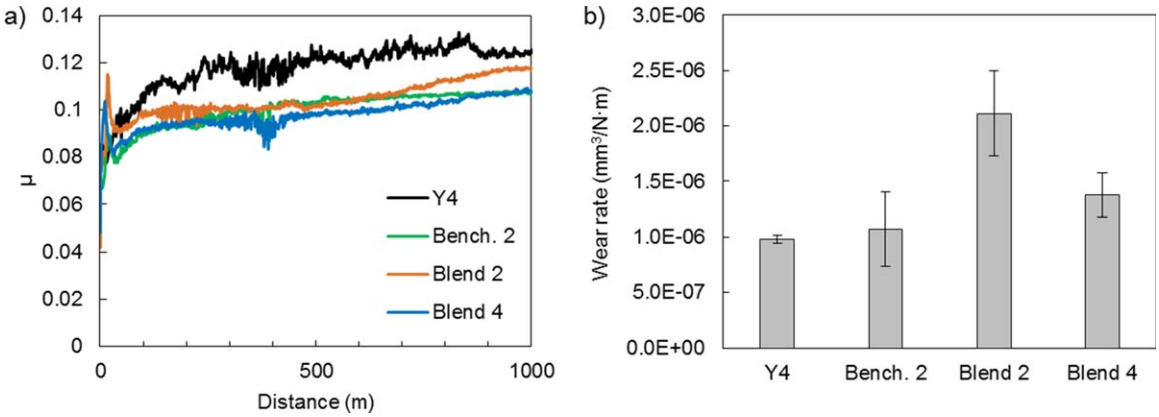

Figure 4. Friction (a) and wear (b) results of boundary lubrication at 100 °C. For each oil, the friction values are the average of two replicates. The wear rates are for the cast iron flats. [Color figure can be viewed in the online issue, which is available at wileyonlinelibrary.com.]

(48.6 − 56.6 cSt) suggesting the friction reduction is mainly a result of composition and structural differences between these materials and not of viscosity. In Figure 3, at 23 °C, benchmark 2 (KV23 = 56.6 cSt) appears to have little influence on the friction versus the neat oil (KV23 = 37.3 cSt). In contrast, analogs 2 − 6 demonstrated a reduction in the friction coefficient (μ) where the greatest reductions were observed for analogs 2 and 4. It is worth mentioning that the friction data of any blended lubricants are not directly comparable unless their respective KVs, at a set temperature, are similar. At room temperature, the KVs between analogs 2 − 6 are comparable with a maximum value difference of 10% suggesting that differences in friction behavior are a result of structural and composition subtleties. For example, although analog 2 contains a bi-modal macromolecule molar mass distribution its KV23 is 52.0 cSt, which is very similar to the KV23 of analog 4 at 53.5 cSt, affording comparable friction results at room temperature. Careful scrutiny of the data supports star-shaped PAMAs with a lower number of arms ($<\alpha^4$) and shorter pendant chains ($\leq PA_{12}MA$) have a more favorable effect on reducing friction. Molecular weight however appears to have the largest influence on friction, as observed in analogs 2 and 4, both of which have the highest $\bar{M}_w^{app}$ and lowest friction. It is possible that high molar weight fractions induce film forming behavior, known to reduce friction.[41] Once again, the viscosity of these blends (2 and 4) at room temperature is less than 2% different from one another and therefore is unlikely to be the culprit that is influencing the friction results. Overall, our analogs appear to have a positive effect in reducing friction as opposed to benchmark 2, particularly analogs 2 and 4 appear to offer unique friction advantages.

The boundary lubrication results at 100 °C also showed a reduction in friction for oils with star-shaped PAMA additives over the neat oil (Y4) and benchmark 2 (Figure 4). Analog 2, and particularly analog 4, appear to have a good friction profile at 100 °C. On the other hand, analog 2 caused a substantial rise in wear whereas analog 4 showed a minor wear increase, relative to Y4 and benchmark 2. This could be indicative of a lower pressure-viscosity coefficient of our additives as compared to the commercial product.[18]

Due to its polar core, analog 4 was expected to have a greater affinity for metal surfaces at elevated temperatures, thus a potential result in friction reduction was envisioned. Indeed, experimental results at both room temperature and 100 °C support this hypothesis, though the superior friction reduction did not translate into improved wear reduction.

CONCLUSIONS

A number of star-shaped homo-PAMAs, with a varying number of arms (3 − 6) and comparable arm lengths were synthesized and their molecular features that may influence viscometric properties of engine oils were evaluated. Our initial goal to prepare an oil-miscible star polymer with competitive lubricant performance to commercial VM was met. Our polymeric materials outperformed benchmark 1 in low temperature viscosity and VI performance parameters. Likewise, friction investigations of star-shaped PAMA reveal more appealing results over benchmark 2. On the other hand, wear rates were observed to mildly increase with our blends.

Furthermore, lubricant performance and molecular features were analyzed to determine any structure–property relationships. The number of arms appeared to have a significant influence on low temperature kinematic viscosity but not on VI. In fact, no clear trend was observed between arm number and VI performance. Arm-length and molecular weight influenced viscosity and VI to a greater extent. For analogs with up to 4-arms, arm-length appeared to contribute to VI behavior, whereas molecular weight was the dominant parameter above 4-arms. Elongating pendant groups had no beneficial effect toward VI values. On the contrary, star polymers with less than 4-arms demonstrated improvements toward reducing friction. Notably, these improvements in friction may have been inspired by star–star coupling (large molecular weight fractions) or a relatively large polar core. The latter did not affect wear rate as adversely as the former suggesting polar groups and topology should be considered further in future structure–property studies.

Overall, these preliminary investigations confirmed the utility of star-shaped PAMAs as VMs and concluded that there is not one molecular feature particularly dominant in influencing lubricant performance. The effects of arm-length, molecular weight, and number of arms are closely intertwined so that it is difficult to decouple their individual contribution. Additional studies would support future designs of VM thereby mitigating engine oil viscosity losses and improve fuel efficiency as well as address environmental stewardship efforts.

ACKNOWLEDGMENTS

This project was funded by the Office of Vehicle Technology (VT) of the U.S. Department of Energy (US DOE), (under contract No. 27573). A portion of this research was performed using EMSL, a national scientific user facility sponsored by the Department of Energy's Office of Biological and Environmental Research and located at Pacific Northwest National Laboratory. PNNL is proudly operated by Battelle for the U.S. DOE (under Contract DE_AC06–76RLO 1830). The authors cordially acknowledge contributions from Anil K. Shukla (PNNL) for performing time-of-flight mass spectrometry and helpful discussions with Ewa Bardasz (Energetics). The authors would like to express their gratitude to David Gray (Evonik) and JoRuetta Ellington (Evonik) for their technical assistance and guidance throughout the project. Authors thank Afton Chemical for generously donating base oils for screening purposes. **Author Contributions**: J.W.R. synthesized and characterized the materials as well as measured viscosity. Y.Z. conducted friction measurements and analyzed results. R.E. conducted high temperature high shear experiments and analyzed results. J.Q. analyzed friction results. L.C. proposed the original concept, original material design, structured collaborations, and analyzed results. All authors reviewed this manuscript.

REFERENCES

1. Otto, M.; Blackwood, D. *Oil Gas J.* **1934**, *33*, 98.
2. Otto, M., Müller-Cunardi, M. (I. G. Farbenindnstrie Aktlengeseilschaft). U.S. Pat. 2,130,507 (**1938**).

3. Thomas, R. M.; Zimmer, J. C.; Turner, L. B.; Rosen, R.; Frolich, P. K. *Ind. Eng. Chem. Res.* **1940**, *32*, 299.
4. Rizvi, S. Q. A. A Comprehensive Review of Lubricant Chemistry, Technology, Selection, and Design; ASTM International: West Conshohocken, **2009**.
5. Covitch, M. J.; Trickett, K. J. *Adv. Chem. Eng. Sci.* **2015**, *5*, 134.
6. ASTM-Standard-D2270-10e1; ASTM International: Standard Practice for Calculating Viscosity Index from Kinematic Viscosity at 40 and 100 °C; ASTM International: West Conshohocken, Pennsylvania, **2011**, www.astm.org.
7. Murphy, C. M.; Zisman, W. A. *Ind. Eng. Chem. Res.* **1950**, *42*, 2415.
8. Wu, M. M.; Ho, S. C.; Forbus, T. R. In Synthetic Lubricant Base Stock Processes and Products, 1st ed.; Hsu, C. S., Robinson, P. R., Eds.; Springer: New York, **2006**; Chapter 17, p 553.
9. Van-Horne, W. L. *Ind. Eng. Chem. Res.* **1949**, *41*, 952.
10. Wang, J. L.; Ye, Z. B.; Zhu, S. P. *Ind. Eng. Chem. Res.* **2007**, *46*, 1174.
11. Stöhr, T.; Eisenberg, B.; Müller, M. *SAE Int. J. Fuels Lubr.* **2008**, *1*, 1511.
12. Sutton, M. R.; Barton, W. R. S.; Price, D. Int. Pat. 2,012,162,207, (**2012**).
13. Johnson, J. R., Schober, B. J. (The Lubrizol Corporation). Int. Pat. 2,014,031,154 (**2014**).
14. Duggal, A. Eur. Pat. 2,444,475 (**2012**).
15. Bruson, H. A. (Haas Company). U.S. Pat. 2,091,627 (**1937**).
16. Janovic, Z.; Saric, K.; Sertic-Bionda, K. *Chem. Biochem. Eng. Q.* **1998**, *12*, 19.
17. Eisenberg, B.; Stöhr, T.; Schimmel, T.; Radano, C. P.; Langston, J. A.; Moore, P. (Evonik RohMax Additives GmbH). Int. Pat. 2,012,076,676 (**2012**).
18. Mary, C.; Philippon, D.; Lafarge, L.; Laurent, D.; Rondelez, F.; Bair, S.; Vergne, P. *Tribol. Lett.* **2013**, *52*, 357.
19. Visger, D. C.; Davies, M.; Price, D.; Baum, M.; Schober, B. J. (The Lubrizol Corporation). U.S. Pat. 200,702,440,18 A1 (**2007**).
20. Wright, P. Ph.D. Thesis, University of Warwick, Coventry England, **2008**.
21. Stoehr, T.; Mueller, M.; Eisenberg, B.; Becker, H.; Mueller, A. (Evonik Rohmax Additives GmbH). U.S. Pat. 8,163,682 B2 (**2012**).
22. Ver Strate, G.; Struglinski, M. J. *Polym. Mater. Sci. Eng.* **1989**, *61*, 252.
23. Fetters, L. J.; Kiss, A. D.; Pearson, D. S.; Quack, G. F.; Vitus, F. J. *Macromolecules* **1993**, *26*, 647.
24. Ebrahimi, T.; Hatzikiriakos, S. G.; Mehrkhodavandi, P. *Macromolecules* **2015**, *48*, 6672.
25. Covitch, M. J. "How Polymer Architecture Affects Permanent Viscosity Loss of Multigrade Lubricants", SAE Technical Paper, **1998**, No. 982638, DOI: 10.4271/982638.
26. Gao, C.; Yan, D. Y.; Zhang, B.; Chen, W. *Langmuir* **2002**, *18*, 3708.
27. Aloorkar, N. H.; Kulkarni, A. S.; Patil, R. A.; Ingale, D. J. *Int. J. Pharm. Sci. Nanotechnol.* **2012**, *5*, 1675.
28. Uniteasy 2008, Available at: www.uniteasy.com/en/unitsCon/calvi.htm (accessed December 1, **2015**).
29. Blau, P. J.; Cooley, K. M.; Bansal, D.; Smid, I.; Eden, T. J.; Neshastehriz, M.; Potter, J. K.; Segall, A. E. *Wear* **2013**, *302*, 1064.
30. Hadjichristidis, N.; Pitsikalis, M.; Pispas, S.; Iatrou, H. *Chem. Rev.* **2001**, *101*, 3747.
31. Kamigaito, M.; Ando, T.; Sawamoto, M. *Chem. Rev.* **2001**, *101*, 3689.
32. Hawker, C. J.; Bosman, A. W.; Harth, E. *Chem. Rev.* **2001**, *101*, 3661.
33. Barner-Kowollik, C.; Davis, T. P.; Stenzel, M. H. *Aust. J. Chem.* **2006**, *59*, 719.
34. Matyjaszewski, K.; Xia, J. H. *Chem. Rev.* **2001**, *101*, 2921.
35. Gao, H. F.; Min, K.; Matyjaszewski, K. *Macromol. Chem. Phys.* **2007**, *208*, 1370.
36. Church, D. C.; Peterson, G. I.; Boydston, A. J. *ACS Macro Lett.* **2014**, *3*, 648.
37. SAE International. **2015**, J300-201501, Available at: http://www.sae.org (accessed October 1, 2015).
38. Covitch, M. J.; Brown, M.; May, C.; Selby, T.; Goldmints, I.; George, D. *SAE Int. J. Fuels Lubr.* **2010**, *3*, 1030.
39. Tamoto, Y. *Jeti* **2004**, *52*, 35.
40. Tang, Z. L.; Li, S. H. *Curr. Opin. Solid State Mater. Sci* **2014**, *18*, 119.
41. Muller, M.; Topolovec-Miklozic, K.; Dardin, A.; Spikes, H. *Tribol. Lubr. Technol.* **2011**, *67*, 50.
42. Smeeth, M.; Spikes, H.; Gunsel, S. *Tribol. Trans.* **1996**, *39*, 726.